PROCEEDINGS, 47th Workshop on Geothermal Reservoir Engineering
Stanford University, Stanford, California, February 7-9, 2022
SGP-TR-223

Time Variations in Velocity and Density in Geothermal Reservoirs

Randall L. Mackie, Wolfgang Soyer, and Stephen Hallinan

CGG Multiphysics, Milan

randall.mackie@cgg.com, wolfgang.soyer@cgg.com, stephen.hallinan@cgg.com

Keywords: Tomography, inversion, seismic, microearthquake, gravity, velocity, density

ABSTRACT

Time-lapse geophysical data at geothermal reservoirs are an important tool for monitoring physical properties important in the production and life of the system; the most commonly used are repeat precision gravity and levelling surveys, and microearthquake (MEQ) receiver networks. The MEQ receiver locations are seldom permanent, however, and with the naturally changing MEQ event locations, the continuously changing seismic ray path coverage complicates the analysis of the time-lapse MEQ data. Standard methods of inverting time-lapse data fall short when faced with simultaneously analyzing both time-lapse microearthquake and time-lapse gravity data. We have therefore developed a new approach for inverting data collected at two different time periods for a baseline model and the changes to that model over the intervening period. Our approach is easily extended to the case of joint inversion of both time-lapse microearthquake and time-lapse gravity data using a cross-gradient link to constrain the model differences. We demonstrate our method on a realistic synthetic data set.

1. INTRODUCTION

A variety of geophysical methods are routinely deployed to explore and develop volcanic-hosted, high enthalpy, geothermal fields including magnetotellurics (MT), gravity, and microearthquake (MEQ) data (Vp and Vs first arrival times). MT is the primary geophysical exploration method since the subsurface resistivity is dependent on primary lithology, secondary (hydrothermal) alteration grade and intensity, temperature, porosity and pore fluid salinity (Ussher et al., 2000; Cumming, 2009). Ground gravity responds to lateral density contrasts such as significant fault systems, vertically oriented intrusive bodies, and/or propylitic-altered density anomalies. During production and development phases, repeat precision gravity and levelling surveys and continuously recording MEQ arrays are increasingly deployed to map time variations in density and seismic velocity (and seismic event distributions) because these reflect rock/fluid interactions, pressure/stress changes, fluid saturation changes, and production versus recharge balances. High enthalpy geothermal systems are typically not exploited using closed-loop binary systems, and so there is a net steam/fluid reduction in rock which is important to monitor with time.

Time-lapse tomography applications include electrical resistivity tomography (ERT, e.g., Van et al, 1991; Hayley et al, 2011; Karaoulis et al, 2013; Lesparre et al, 2017) and seismic tomography (e.g., Vesnaver et al, 2003; Julian and Folger, 2010; Qian et al, 2018). When the data measurement system is permanently installed over the course of the experiment, then it is straightforward to image time variations by tomographic inversion of the differences in observed data between different time periods, as is often done in the case of time-lapse ERT (see for example, Hayley et al, 2011).

If, however, the data measurement system is not permanently installed and the locations of the sources and receivers change with time, then the problem of imaging property variations over time is much more difficult. This is typically the case for geophysical data collected at geothermal fields, such as MEQ data, where seismic receivers are moved depending on where active injection and production is being carried out, and the sources, which are microearthquakes caused by injection. This is the problem we consider in this work, that is, how to image the time variations of physical properties in a geothermal reservoir by tomographic analysis of data collected at different times (baseline and monitoring data) and where receivers are moved around and the source field (in the case of MEQs) changes.

2. METHOD

The standard approach to solving nonlinear geophysical inverse problems is by regularized least-squares, in which the solution is taken to be the minimum of an objective function of the form

$$\Psi(m) = \big(d - F(m)\big)^T W\big(d - F(m)\big) + \lambda(m - m_0)^T K(m - m_0), \tag{1}$$

where d is the observed data vector, F is the forward modeling function, m is the unknown model vector, W is a weighting matrix (usually the inverse variance or covariance), λ is the regularization parameter, K is a discrete form of a stabilizing smoothing function, and m_0 is an (optional) a priori model. There are many ways to solve the numerical (and nonlinear) optimization problem described by equation (1) such as Gauss-Newton and nonlinear conjugate gradients (Rodi and Mackie, 2001).

The simplest approach to analyzing time-lapse data is to carry out an inversion for each dataset collected at different times and then difference the models. However, this approach is prone to be problematic because noise in different data sets can be propagated into the individual inversion results and thus contaminate the difference models (Hayley et al, 2011). A slightly more sophisticated approach is

called the cascaded time-lapse inversion approach (Miller et al, 2008) in which the result of inverting the data at the starting time is used as the starting and *a priori* models for the subsequent data. This basically is solving for the variations away from the *a priori* model that fit the data at the subsequent time period and thus strives to keep the two models close.

In the case where the measurement system does not change (that is, the sources and receivers are fixed in a permanent installation), then one can use the same inversion algorithm used to solve equation (1) by simply changing the residual vector from $(d - F(m))$ to $[(d_2 - d_1) - (F(m_2) - F(m_1))]$ and solving directly for the model variations between the models over the intervening time period. This is called a difference inversion algorithm by LaBrecque and Yang (2000) and requires solving first for the background model m_1 using the data d_1 at the initial state. Further approaches are discussed in Haley et al (2011), for example.

We are particularly interested, however, in the situation where a permanent monitoring installation is not available and instead measurements (and sources) are moved between data acquisitions. One can follow the simplest approach mentioned above and carry out a tomographic analysis of the data from each time period separately and compare the results with the assumption that all changes arise from time variations in the velocity. Foulger et al (1997) carried out such analysis for a permanent network to analyze the temporal variations from data collected at the Geysers geothermal field from 1991 and 1994. With temporal changes in the seismic network in addition to the variability of MEQs and therefore increased changes in the seismic ray distribution, this approach is more problematic.

Julian and Foulger (2010) proposed a different approach whereby data from two different time periods are inverted simultaneously with an additional constraint added to the objective function to minimize the differences between the two models. In our tests on synthetic and real data, we found this method worked reasonably well, although it takes some trial and error to determine the optimal regularization parameter that weights the similarity of the two models.

Our work herein was motivated by the desire to jointly invert both MEQ data and gravity data and solve for the model differences while simultaneously constraining the velocity and density changes to be structurally similar using the cross-gradient approach of Gallardo and Meju (2003). We therefore propose a new algorithm in which data from two different time periods are inverted simultaneously, but instead of inverting for two models (m_1 and m_2) with a closeness constraint (or some variation thereof), we invert directly for m_1 and the changes in the model Δm, namely,

$$d_1 = F(m_1), \tag{2a}$$

$$d_2 = F(m_1, \Delta m), \tag{2b}$$

$$m_2 = m_1 + \Delta m. \tag{2c}$$

The objective function in equation (1) is expanded to include misfits for d_1 and d_2, as well as regularization terms for m_1 and Δm. For convenience, let $r = (d - F(m))$, and ignoring dependence on an *a priori* model, then we can write the expanded objective function as

$$\Psi(m_1, \Delta m) = r_1^T W_1 \mathrm{r}_1 + r_2^T W_2 \mathrm{r}_2 + \lambda_1 m_1^T K_1 m_1 + \lambda_2 \Delta m^T K_2 \Delta m, \tag{3}$$

where r_1 and r_2 are the residuals in the data at two different time periods and regularization (smoothing) is applied to both m_1 and Δm. There are many advantages to setting up the inversion this way to solve directly for the initial model and the changes to that model: (1) data from both time periods logically determine the background model while only the data from the second time period determines the temporal changes, (2) there are no assumptions about model geometry or distribution of sources/receivers, (3) parameterizing the inversion directly in terms of Δm immediately allows joint inversion with time-lapse gravity data for density variations and the ability to constrain the velocity and density changes to be structurally similar by inclusion of a cross-gradient constraint (Soyer et al, 2018). In this case, we can write the objective function as, where now we make explicit that we are inverting for $v_1, \Delta v, \Delta\rho$,

$$\Psi(v_1, \Delta v, \Delta\rho) = r_1^T W_1 \mathrm{r}_1 + r_2^T W_2 \mathrm{r}_2 + r_g^T W_g \mathrm{r}_g + \lambda_1 v_1^T K_1 v_1 + \lambda_2 \Delta v^T K_2 \Delta v + \lambda_3 \Delta\rho^T K_3 \Delta\rho + \lambda_{xg} \varphi_{xg}^2, \tag{4}$$

where r_1 and r_2 are the residuals in seismic baseline and monitoring data, v_1 is the baseline velocity model, Δv is the change in velocity, $\Delta\rho$ is the change in density, r_g is the gravity residual, and where we have added an additional smoothing regularization term for density changes $\Delta\rho$ and we have added a cross-gradient constraint between Δv and $\Delta\rho$. The numerical example shown in the next section is based on the solution of this minimization problem.

3. EXAMPLE

The concept was tested on a synthetic setup, inspired by a real geothermal monitoring case in terms of receiver and event locations and available P/S travel time picks. About 2,600 and 3,000 events are available respectively for epoch 1 and 2 (baseline and monitoring data), measured at a total of 18 receiver locations with only partially overlap between epochs, and where not all receivers are active throughout the respective time period. The MEQ events are recorded at only 4 to 12 receivers, and fewer S than P wave travel times are available (85% and 50% for epoch 1 and 2, respectively). In addition to the seismic monitoring, gravity time-lapse data are simulated at ~70 benchmark locations.

Forward data were calculated for synthetic models using a finite difference solution of the eikonal equation based on Noble et al (2014). The synthetic models were derived from a background 3D velocity model with a predominantly vertical gradient plus minor lateral variations, and where the velocity inside a defined "reservoir" zone was a) raised by 5% above background in epoch 1 and b) lowered by 5% below background in epoch 2, both for Vp and Vs, thus generating a 10% change between the two epochs within the reservoir (Figure

1). Density was modelled as a decrease between epochs by -0.01g/cc inside the reservoir zone (not illustrated). These property changes are considered illustrative, rather than necessarily representative of a real case. A Gaussian error with a mean of 25 (*1.65) msec was added to the synthetic P (S) travel times, and a mean 150m random error was added in each dimension to the MEQ hypocenter locations, which besides the precise time of an event is another unknown for real data MEQ tomography. Likewise, a mean 0.015mGal random error was added to the synthetic gravity data.

The inversion results presented here (Figures 2 to 5) are from a joint inversion for several model parameters: (1, 2) Vp and Vs for both epochs, (3) MEQ event location updates, and (4) the density property change – all estimated here from a single inversion run. Inversions started from the background velocity models and zero density (= no change). Cross-gradient structural similarity constraints were used between Δv_p & Δv_s, and also between Δv_p & density and Δv_s & density, using different weights. The *a priori* model for Δv is taken to be zero, thus imposing the condition to make the variations as small as possible.

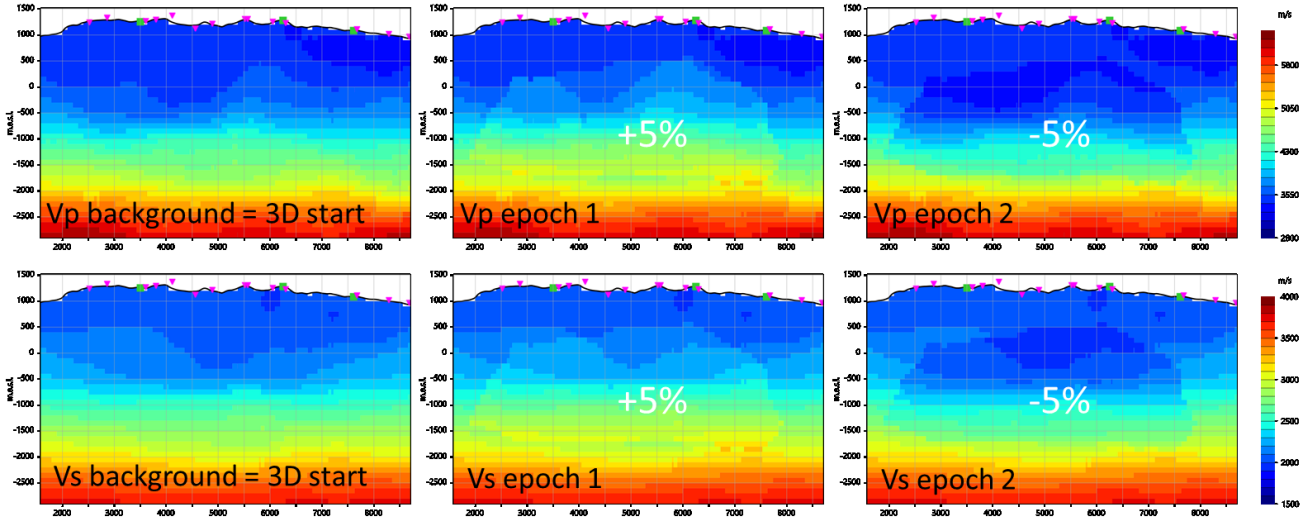

Figure 1: Slice through velocity models used in the synthetic setup. Both Vp and Vs were raised (center) and lowered (right) by 5% with respect to the 3D background model (left).

The inverted property volumes recover the input volumes fairly well, and the inversion model responses reproduce the input data with a root mean square (RMS) of 0.97-0.98 (traveltimes) and 1.38 (gravity). The higher gravity misfit is due to a relatively high structural (smoothing) constraint on density, to avoid a shallower concentration of modelled density changes that are typical of density inversions.

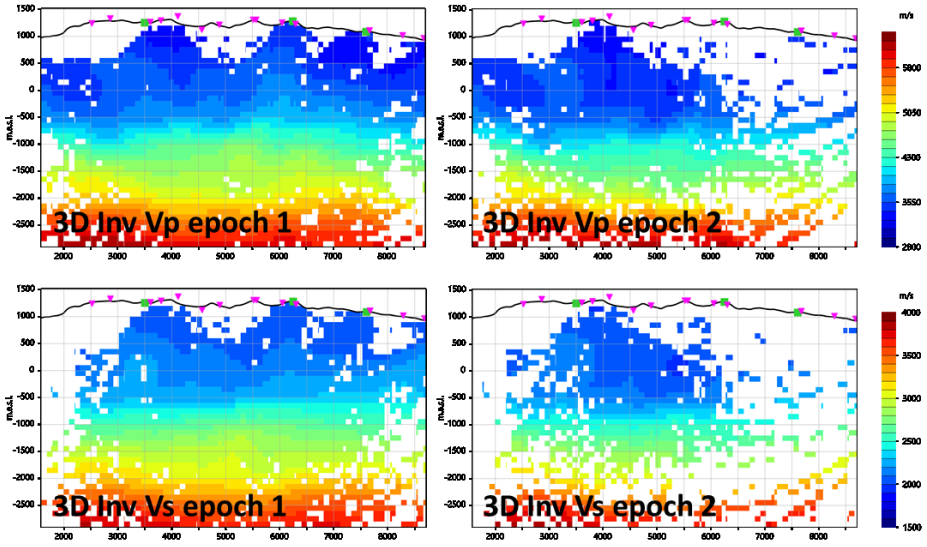

Figure 2. Slices through the velocity models recovered by the joint inversion: Vp (top) and Vs (bottom), epochs 1 (left) and 2 (right). Only cells with sufficient 3D illumination are shown.

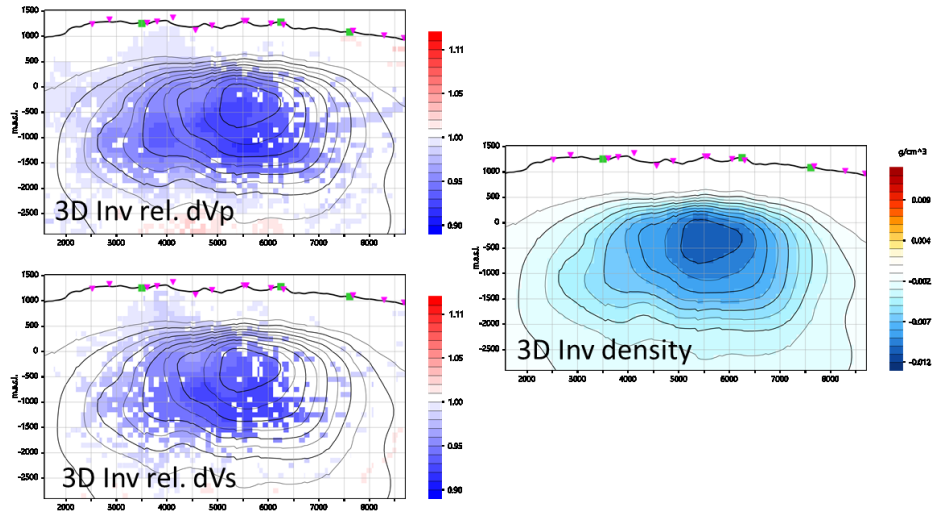

Figure 3: Relative velocity changes, from division of the epoch velocity models (2/1), for both Vp (top) and Vs (bottom), and inverted density change (right). Density change contours are also shown in black on the velocity changes. Only cells with sufficient 3D illumination are shown.

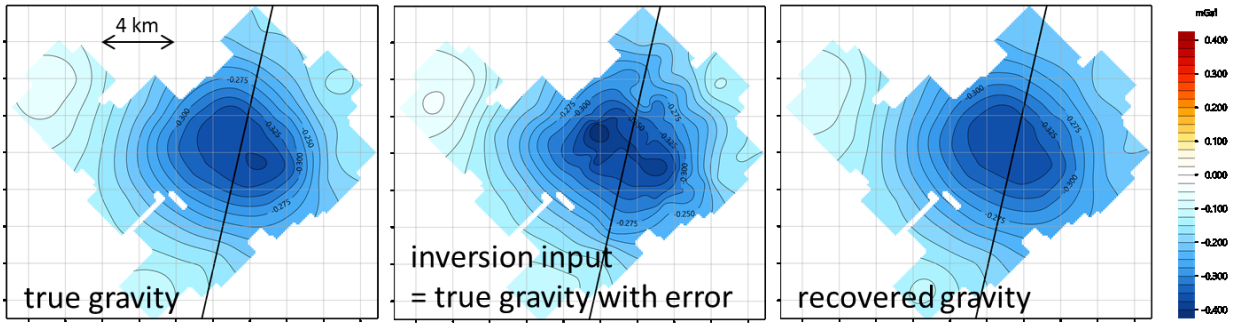

Figure 4: Gravity data fit of the joint inversion. An error of 0.0.15mGal was added to the response of the true model.

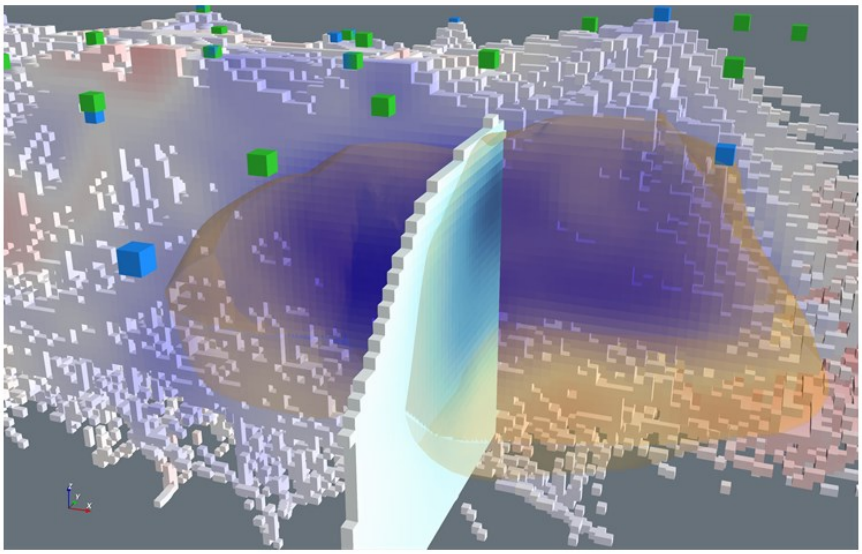

Figure 5: 3D view of the modelled relative Vp change between epochs (half volume) and the absolute density change (single slice). The closed reservoir surface is shown in transparent orange. Only cells with sufficient 3D illumination are shown. Color scale as in previous figures.

4. CONCLUSIONS

We have implemented a new algorithm for inverting time-lapse geophysical data, which is parameterized in terms of the initial background model and the changes in the model property (m_1 and Δm). The many advantages over previous approaches include parameterization directly in terms of the model changes with no assumptions about the data geometry at different time periods. It is suited particularly well, therefore, to inverting time-lapse MEQ data from changing seismic receiver arrays as well as the varying MEQ source locations. Furthermore, this approach facilitates simultaneous joint inversion of the MEQ data with other time lapse datasets such as repeat precision gravity and levelling surveys, using a cross-gradient constraint to impose structural similarity between changes in properties. We have applied the algorithm to synthetic data using realistic model and data geometries, inspired by the issues raised in a real data case.

While the algorithm works well for non-static seismic receiver arrays, we should stress that for such sparse seismic networks a permanent installed network has tremendous advantages in the analysis of velocity variations from time-lapse MEQ data.

REFERENCES

Foulger, G.R., Grant, C.C., Ross, A., and Julian, B.R.: Industrially Induced Changes in Earth Structure at The Geysers Geothermal Area, California, Geophysical Research Letters, 24, (1997), 135-137.

Gallardo, L.A., and Meju, M.A.: Characterization of Heterogeneous Near-Surface Materials by Joint 2D Inversion of DC Resistivity and Seismic Data, *Geophysical Research Letters*, 30, (2003), 1658.

Hayley, K., Pidlisecky, A., and Bentley, L.R.: Simultaneous Time-Lapse Electrical Resistivity Inversion, Journal of Applied Geophysics, 75, (2011), 401– 411.

Julian, B.R., and Foulger, G.R.: Time-Dependent Seismic Tomography, Geophysical Journal International, 182, (2010), 1327-1338.

Karaoulis, M., Tsourlos, P., Kim, J-H., and Revil, A.: 4D Time-Lapse ERT Inversion: Introducing Combined Time and Space Constraints, Near Surface Geophysics, 11, (2013).

LaBrecque, D.J. and Yang, X.: Difference Inversion of ERT Data: a Fast Inversion Method for 3-D In Situ Monitoring, Journal of Environmental and Engineering Geophysics, 6, (2001), 83-89.

Lesparre, N., Nguyen, F., Kemna, A., Robert, T., Hermans, T., Daoudi, M., and Flores-Orozco, A.: A New Approach for Time-Lapse Data Weighting in Electrical Resistivity Tomography, Geophysics, 82, (2017), E325-E333.

Miller, C.R., Routh, P.S., Brosten, T.R., and McNamara, J.P.: Application of Time-Lapse ERT Imaging to Watershed Characterization, Geophysics, 73, (2008), G7-G17.

Noble, M., Gesret, A., and Belayouni, N.: Accurate 3-D Finite Difference Computation of Traveltimes in Strongly Heterogenous Media, Geophysical Journal International, 199, (2014), 1572-1585.

Qian, J., Zhang, H., and Westman, E.: New Time-Lapse Seismic Tomographic Scheme Based on Double-Difference Tomography and its Application in Monitoring Temporal Velocity Variations Caused by Underground Coal Mining, Geophysical Journal International, 215, (2018), 2093-2104.

Rodi, W. and Mackie, R.L.: Nonlinear Conjugate Gradients Algorithm for 2-D Magnetotelluric Inversion, Geophysics, 66, (2001), 174-187.

Soyer, W., Mackie, R.L., Hallinan, S., Pavesi, A., Nordquist, G., Suminar, A., Intani, R. and Nelson, C.: Geologically-consistent Multiphysics Imaging of the Darajat Geothermal Steam Field, *First Break*, 36, (2018), 77-83.

Ussher, G., Harvey, C., Johnstone, R., and Anderson, E.: Understanding the Resistivities Observed in Geothermal Systems, *Proceedings, World Geothermal Congress*, Kyushu-Tohoku, Japan (2000).

Van, G.P., Park, S.K., and Hamilton, P.: Monitoring Leaks from Storage Ponds Using Resistivity Methods, Geophysics, 56, (1991), 1267-1270.

Vesnaver, A.L., Accaino, F., Bohm, G., Madrussani, G., Pajchel, J., Rossi, G., and Dal Moro, G.: Time-Lapse Tomography, Geophysics, 68, (2003), 815-823.